



HAL
open science

Deletion of the RNA-binding proteins Zfp36l1 and Zfp36l2 leads to perturbed thymic development and T-lymphoblastic leukaemia.

Martin Turner, Daniel James Hodson, Michelle Louise Janas, Alison Galloway, Simon Andrews, Cheuk Li, Richard Pannell, Christian William Siebel, Hugh Robson Macdonald, Kim de Keersmaecker, et al.

► To cite this version:

Martin Turner, Daniel James Hodson, Michelle Louise Janas, Alison Galloway, Simon Andrews, et al.. Deletion of the RNA-binding proteins Zfp36l1 and Zfp36l2 leads to perturbed thymic development and T-lymphoblastic leukaemia.. Nature Immunology, 2010, 10.1038/ni.1901 . hal-00554655

HAL Id: hal-00554655

<https://hal.science/hal-00554655>

Submitted on 11 Jan 2011

HAL is a multi-disciplinary open access archive for the deposit and dissemination of scientific research documents, whether they are published or not. The documents may come from teaching and research institutions in France or abroad, or from public or private research centers.

L'archive ouverte pluridisciplinaire **HAL**, est destinée au dépôt et à la diffusion de documents scientifiques de niveau recherche, publiés ou non, émanant des établissements d'enseignement et de recherche français ou étrangers, des laboratoires publics ou privés.

1 **Deletion of the RNA-binding proteins *Zfp36l1* and *Zfp36l2* leads to**
2 **perturbed thymic development and T-lymphoblastic leukaemia.**
3

4 Daniel J. Hodson¹, Michelle L. Janas¹, Alison Galloway¹, Sarah E. Bell¹, Simon Andrews²,
5 Cheuk M. Li¹, Richard Pannell³, Christian W. Siebel⁴, H. Robson MacDonald⁵, Kim De
6 Keersmaecker⁶, Adolfo A. Ferrando^{6,7,8}, Gerald Grutz^{9,10} and Martin Turner¹.

7
8 ¹Laboratory of Lymphocyte Signalling and Development, ²Bioinformatics Group, The
9 Babraham Institute, Babraham, Cambridge, CB22 3AT, United Kingdom. ³MRC Laboratory
10 of Molecular Biology, Hills Road, Cambridge CB2 0QH, UK ⁴Genentech, Department of
11 Molecular Biology, 1 DNA Way, South San Francisco, CA 94080 USA. ⁵Ludwig Institute for
12 Cancer Research, Lausanne Branch, University of Lausanne, 1066 Epalinges, Switzerland.
13 ⁶Institute for Cancer Genetics, Columbia University Medical Centre, New York, USA.
14 ⁷Department of Pathology, Columbia University Medical Centre, New York, USA. ⁸
15 Department of Pediatrics, Columbia University Medical Centre, New York, USA. ⁹Institute of
16 Medical Immunology, Charité-Universitätsmedizin, Campus Mitte, Berlin, Germany. ¹⁰Center
17 for Biomaterial Development, Institute of Polymer Research, GKSS, Teltow, Germany.

18
19
20
21 * Correspondence should be addressed to M.T. (martin.turner@bbsrc.ac.uk). Laboratory of
22 Lymphocyte Signalling and Development, The Babraham Institute, Babraham, Cambridge
23 CB22 3AT, United Kingdom. tel +44 (0)1223 496403. fax +44(0)1223 496023

24 **ZFP36L1 and ZFP36L2 are RNA-binding proteins (RBPs) which interact with AU-rich**
25 **elements in the 3'UTR of mRNA, leading to mRNA degradation and translational**
26 **repression. Mice lacking ZFP36L1 and ZFP36L2 during thymopoiesis develop a**
27 **Notch1-dependent T cell acute lymphoblastic leukaemia (T-ALL). Prior to the onset of**
28 **T-ALL, thymic development is perturbed with accumulation of cells which have**
29 **passed through the β -selection checkpoint without first expressing T cell receptor**
30 **β (TCR- β). Notch1 expression is increased in non-transformed thymocytes in the**
31 **absence of ZFP36L1 and ZFP36L2. Both RBPs interact with evolutionarily conserved**
32 **AU-rich elements within the 3' untranslated region of Notch1 and suppress its**
33 **expression. These data establish a role for ZFP36L1 and ZFP36L2 during thymocyte**
34 **development and in the prevention of malignant transformation.**

35

36 The development of T cells in the thymus proceeds through a series of developmental
37 stages characterised by progressive rearrangement of the T cell receptor (TCR) genes and
38 regulated by a series of developmental checkpoints. This ordered process is orchestrated
39 by transcription factor networks which integrate environmental cues to initiate gene
40 expression programs appropriate to the developmental stage of the thymocyte¹⁻³. However
41 there is increasing recognition that gene expression during lymphocyte development is also
42 subject to regulation by post-transcriptional mechanisms. These affect the half-life of mRNA
43 through promotion or inhibition of mRNA decay. Additional control at the point of mRNA
44 translation also regulates the magnitude of gene expression. These points are exemplified
45 by recent awareness of the regulation of gene expression by microRNAs which act
46 principally through the control of mRNA decay and translation. Post-transcriptional control of
47 gene expression is also mediated by RNA-binding proteins (RBPs) of which over 150 have
48 been found to be expressed in thymus⁴. However, our knowledge of how post-
49 transcriptional regulation mediated by RNA-binding proteins impacts on thymic development
50 is extremely limited.

51 ZFP36L1 and ZFP36L2 (also known as TIS11b and TIS11d) belong to a family of CCCH-
52 zinc finger-containing RBPs that includes ZFP36 (tristetraprolin). These regulate gene
53 expression by promoting mRNA decay and might additionally affect translation. A germline
54 *Zfp36* knockout mouse develops a severe inflammatory phenotype attributable to
55 overexpression of TNF⁵⁻⁶ while germline knockout of *Zfp36l1* is lethal at embryonic day 10.5
56 due to a failure of chorioallantoic fusion⁷⁻⁸. Germline *Zfp36l1* knockout mice die shortly after
57 birth possibly as a consequence of haematopoietic stem cell failure⁹. The tandem zinc
58 fingers are highly conserved between TTP family members and bind to AU-rich elements

59 (ARE) in the 3'-untranslated region (3'UTR) of mRNA, promoting deadenylation and decay.
60 The optimum binding sequence for all family members is UUAUUUUAU¹⁰⁻¹¹. However
61 sequences as short as UAUUU may be sufficient for binding and genome-wide screens to
62 identify targets have been enriched with transcripts that do not possess the optimal AU-rich
63 binding site¹². Thus the criteria for target recognition, and whether this differs between the
64 family members, remain incompletely defined.

65

66 There is mounting evidence that escape from post-transcriptional regulation of gene
67 expression is important in the pathogenesis of malignancy. Deletion of the miR15a &
68 miR16-1 cluster in mice leads to development of a disease similar to human chronic
69 lymphocytic leukaemia¹³. Aberrant polyadenylation site usage, leading to a truncated
70 3'UTR, has been detected in many human malignancies and might allow malignant cells to
71 escape regulation by both microRNA and RBPs¹⁴⁻¹⁵. As a physiological mechanism,
72 proliferating T cells preferentially utilise truncated 3'UTRs¹⁶. This is consistent with a global
73 reduction in post-transcriptional regulation providing a net proliferative advantage.
74 Circumstantial evidence implicates ZFP36 family members in malignancy. Expression of
75 ZFP36 is suppressed in a variety of human malignancies¹⁷. ZFP36L2 has been suggested
76 to act downstream of p53 in the induction of apoptosis and ZFP36L1 is implicated in the
77 apoptotic response to rituximab (anti-CD20) in chronic lymphocytic leukaemia¹⁸⁻¹⁹. A
78 number of oncogenes, including *FOS*, *MYC*, *BCL-2*, and *COX-2* contain AREs in their
79 3'UTRs and have been proposed as potential targets²⁰. However no evidence to date
80 proves an *in vivo*, physiological tumor suppressor role for ZFP36 family members, or indeed
81 any RBP.

82

83 To investigate the function of ZFP36L1 and ZFP36L2 in thymic development we generated
84 conditional knockouts of both genes. In anticipation of redundancy between these two
85 closely related family members we inter-crossed the single knockouts to create lymphocyte
86 conditional *Zfp36l1* and *Zfp36l2* double knockout (dKO) mice. Thymic development was
87 normal in the single knockouts, however the dKO mice developed T-lymphoblastic
88 leukaemia T-ALL). Prior to leukaemia the normally ordered process of thymic development
89 was perturbed, with aberrant passage of thymocytes through the β -selection checkpoint.
90 Furthermore the oncogenic transcription factor *Notch1* was identified as a novel target of
91 ZFP36L1 and ZFP36L2. The finding that a transcription factor is itself a target for post-
92 transcriptional regulation, demonstrates how RBPs integrate gene expression at the

93 transcriptional and post-transcriptional level. These findings identify a critical role for ZFP36
94 family members during lymphocyte development and provide the strongest evidence to date
95 for their function as tumor suppressors.

96

98 Results

99

100 Double knockout mice develop T-ALL.

101 *Zfp361/1* and *Zfp361/2* are expressed throughout thymic development, especially during the
102 early CD4⁻CD8⁻ double negative stages (**Supplementary Fig. 1**). To examine their function
103 conditional knockout mice were generated using standard gene targeting techniques
104 (**Supplementary Fig. 2**). Mice were inter-crossed and bred to homozygosity for the floxed
105 alleles of both *Zfp361/1* and *Zfp361/2*. Transgenic expression of Cre under the control of a *CD2*
106 locus control region was used to effect deletion prior to the double negative 1 (DN1) stage of
107 thymic development²¹⁻²². Unless otherwise stated control mice were *Zfp361/1^{fl/fl}Zfp361/2^{fl/fl}*.
108 We confirmed that the expression of the *CD2-Cre* transgene alone caused no associated
109 defect in thymic development (data not shown). *Zfp361/1^{fl/fl}Zfp361/2^{fl/fl}CD2Cre* mice, hereafter
110 referred to as double knockout (dKO) for simplicity, were born at expected Mendelian ratios
111 and appeared healthy in early life. However, 90% of dKO mice died or were humanely
112 culled due to ill health by six-months of age (**Fig. 1a**). All of these mice had developed
113 thymic tumors and many also showed splenomegaly and lymphadenopathy
114 (**Supplementary Fig. 3**). Tumor development was never observed in *Zfp361/1^{fl/fl}CD2-Cre* or
115 *Zfp361/2^{fl/fl}CD2-Cre* single mutant mice, or in any intermediate combination of genotypes (e.g.
116 *Zfp361/1^{fl/fl}Zfp361/2^{fl/+}CD2-Cre*). Thus a single allele of either *Zfp361/1* or *Zfp361/2* appeared
117 sufficient to prevent tumor development. All thymic tumors showed high CD8 expression,
118 with variable CD4 expression (**Fig. 1b**). Tumor cells expressed high amounts of heat stable
119 antigen (CD24) but did not express surface T cell receptor beta (sTCR-β). Most, but not all
120 tumors, expressed intracellular TCR-β (icTCR-β). Circulating lymphoblasts were seen upon
121 examination of the peripheral blood (**Fig. 1c,d**). Flow cytometric analysis of spleen, lymph
122 node and bone marrow frequently demonstrated involvement by tumor cells of identical
123 phenotype to the associated thymic tumor (**Fig 1e**). Clonality testing by PCR across the
124 TCR-β2 region suggested that thymic tumors were predominantly oligoclonal (**Fig. 1f**).
125 Taken together, these findings suggest that deletion of *Zfp361/1* and *Zfp361/2* together leads to
126 the development of T-ALL corresponding to the CD8 immature single positive (CD8iSP) and
127 double positive (DP) stages of thymic development.

128

129 Perturbed thymopoiesis prior to tumor development

130 In dKO mice, tumor development was preceded by thymic atrophy. At three and eight
131 weeks of age total thymic cellularity was approximately 50% that of control mice (**Fig. 2a,b**).
132 This atrophic stage was associated with the gradual expansion of the CD8iSP population

133 (CD8⁺CD4⁻CD24^{hi}TCRβ⁻). By thirteen weeks this population was markedly expanded in
134 both proportion and absolute number (**Fig. 2c,d**). Abnormal development was also
135 observed at the CD4⁻CD8⁻ (DN) stages (**Fig. 2e**). The expression of CD44 and CD25 are
136 used to describe four stages of DN development and appeared to show a reduced
137 progression from DN2 (CD44⁺CD25⁺) to DN3 (CD44⁻CD25⁺) (**Fig. 2e**). However the utility of
138 this staining strategy to describe functional progression in the face of perturbed thymic
139 development is limited. Therefore, we examined the expression of intra-cellular TCR-β
140 (icTCR-β) which normally becomes expressed during the DN3 stage following successful
141 TCR-β rearrangement. In dKO mice the proportion of DN thymocytes expressing icTCR-β
142 was markedly reduced (**Fig. 2e & Supplementary Fig. 4**). In wild-type mice the expression
143 of icTCR-β is a prerequisite for cells to pass the β-selection checkpoint. However in dKO
144 mice these icTCR-β⁻ cells displayed features of metabolic activation normally only seen
145 following β-selection. The expression of the amino acid transporter CD98 and the transferrin
146 receptor CD71 is normally low prior to β-selection but increases in a Notch1-dependent
147 manner following β-selection as cellular metabolism increases²³. However expression of
148 CD98 and CD71 was high in all DN thymocytes from dKO mice suggesting metabolic
149 activation even in icTCR-β⁻ thymocytes. (**Fig. 2e**). Consistent with this, icTCR-β⁻ dKO cells
150 showed elevated forward scatter typical of blasting cells (data not shown). Furthermore,
151 cellular proliferation was elevated, as judged by increased uptake of EdU following pulse
152 administration (**Supplementary Fig. 5**). Thus it appeared that dKO thymocytes were able to
153 transit the β-selection checkpoint, with associated metabolic activation and proliferation, but
154 without expression of TCR-β. This aberrant passage through β-selection was associated
155 with differentiation of icTCRβ⁻ thymocytes to the CD8iSP and DP developmental stages
156 which lie downstream of β-selection. As expected, in control mice all thymocytes from the
157 CD8iSP and DP stages expressed icTCR-β. However, in dKO thymocytes, icTCR-β was
158 expressed by only 30% of CD8iSP (**Fig. 2e & Supplementary Fig. 4**). This increased to
159 90% of DP and 100% at the CD4 and CD8 mature single positive (CD8mSP) stages
160 (**Supplementary Fig. 4**). Thus although dKO icTCR-β⁻ cells were able to pass β-selection
161 they were unable to progress beyond the DP stage. Despite the accumulation of TCRβ⁻
162 CD8iSPs, the majority of thymic tumors corresponded to TCRβ⁺ CD8iSP thymocytes
163 suggesting the importance of preTCR signals during leukaemia development.

164

165

166 **Elevated Notch1 expression in dKO thymocytes**

167 We hypothesised that the thymic phenotype observed in dKO mice might result from the
168 over-expression of one or more genes normally suppressed by ZFP36L1 or ZFP36L2. We

169 performed microarray analysis upon whole thymus from control and dKO mice, aged five
170 weeks old and nine weeks old, as this was prior to the development of tumor and, at five
171 weeks of age, the relative thymic proportions were normal, as judged by CD4 and CD8
172 staining (**Fig. 1a**). At nine weeks of age more than 500 significantly changing genes were
173 elevated more than 1.5 fold. Fewer were elevated at five weeks. When the list was filtered
174 to include only genes elevated in both the five week and the nine week arrays, 17 named
175 genes were identified (**Fig. 3a**). Of these 17 up-regulated genes, we chose to investigate
176 further the expression of *Notch1* as this gene is critical for thymic development and in the
177 pathogenesis of T-ALL²⁴. Elevation of mRNA encoding Notch1 and its target genes, *Hes1*,
178 *Myc* and *Dtx1*, was confirmed by real time PCR (**Fig. 3b**). We also showed strong
179 expression of Notch1 protein in thymic tumors, both by immunoblot and flow cytometry (**Fig.**
180 **3c,d**). Notch1 expression by flow cytometry was between 5- and 50-fold higher in thymic
181 tumor than in control thymus (**Fig. 3d**). Notch1 staining was higher in thymic tumor than any
182 individual subpopulation of control thymus suggesting that the elevated tumor expression did
183 not merely reflect an expansion of immature populations (**Fig. 3e**). We also examined
184 Notch1 expression in individual thymic subsets in mice prior to the development of tumor. In
185 mice aged three weeks old, Notch1 expression was elevated at the DN stages. Elevated
186 Notch1 expression was seen in both CD25⁺icTCR-β⁻ and in CD25⁺icTCR-β⁻ DN thymocytes
187 (**Fig. 3f**). Elevated Notch1 expression was also seen at the CD8iSP stage. In dKO mice,
188 both icTCR-β⁺ and icTCR-β⁻ CD8iSP populations highly expressed Notch1 (**Fig. 3g**). Thus
189 Notch1 was abnormally elevated in both DN and CD8iSP thymocytes from dKO mice prior to
190 the onset of T-ALL. This high expression of Notch1 is increased even further in dKO tumor
191 cells.

192

193 **Notch1 is a target of ZFP36L1 and ZFP36L2**

194 The 1.6Kb *Notch1* 3'UTR contains a region of particularly high interspecies conservation
195 within the 300bp following the translation termination codon (**Fig. 4a**). Within this highly
196 conserved region (HCR), the greatest interspecies conservation is clustered into three short
197 regions. Strikingly each of these contains a predicted ZFP36L1 and ZFP36L2 binding site
198 (**Fig. 4b**). These binding sites are not found elsewhere in the *Notch1* 3'UTR. When we
199 examined the 3'UTRs of all 17 genes up-regulated in the microarray, *Notch1* was the only
200 gene to contain the nonameric ARE considered to be the optimum binding site for ZFP36L1
201 and ZFP36L2. To determine whether the *Notch1* 3'UTR could mediate suppression by
202 ZFP36L1 or ZFP36L2 we introduced the complete *Notch1* 3'UTR downstream of the
203 luciferase coding region in pSI-Check2. When this reporter was transfected into HEK293T
204 cells (which do not constitutively express *Zfp36l1* or *Zfp36l2*) the co-transfection of either
205 *Zfp36l1* or *Zfp36l2* suppressed luciferase activity in a dose dependent manner (**Fig. 4c and**

206 **d)** This effect required functional RNA-binding zinc fingers of *Zfp36l1*, as a mutant version
207 of *Zfp36l1* in which both fingers were mutated and which could no longer bind RNA, failed to
208 suppress the *Notch1* UTR reporter (**Fig. 4c**). Furthermore, a reporter containing only the
209 HCR was suppressed by *Zfp36l1* and *Zfp36l2* but these had no effect upon a reporter
210 containing the remainder of the UTR lacking the HCR. In all of these assays expression of
211 ZFP36L1, ZFP36L2 and tandem zinc finger mutant (TZFM) was confirmed by immunoblot
212 (data not shown). To demonstrate a direct physical interaction between ZFP36L1 or
213 ZFP36L2 and the *Notch1* 3'UTR we used a radiolabelled probe (corresponding to 61
214 nucleotides of the *Notch1* 3'UTR containing the nonameric binding site) in an electromobility
215 shift assay (EMSA). Lysate from HEK293T cells transfected with empty pCDNA3 or with
216 pCDNA3-*ZFP36L1*-TZFM expression vector failed to retard the migration of the probe. By
217 contrast, lysates from pCDNA3-*ZFP36L1*, or pCMV2-*ZFP36L2* transfected cells yielded a
218 probe complex with retarded mobility indicative of a direct interaction (**Fig. 4e**). The size of
219 these complexes correlated with the molecular weight of ZFP36L1 (36kDa) and ZFP36L2
220 (50kDa).

221

222 Taken together these results indicate a direct interaction between ZFP36L1 and ZFP36L2
223 with the HCR of the *Notch1* 3'UTR and that this interaction mediates a suppressive effect
224 upon gene expression.

225

226

227 **Infrequent Notch1 mutation in dKO mutant tumors**

228 Mutation of the PEST domain of *NOTCH1* is frequently found in human and mouse models
229 of T-ALL and renders Notch1 protein resistant to degradation. Mutation of the
230 heterodimerisation (HD) domain is also observed and leads to spontaneous cleavage of
231 Notch1 leading to ligand independent signaling activity²⁵. We consider it likely that the
232 absence of ZFP36L1 and ZFP36L2 explains the elevation of Notch1 observed in thymocytes
233 prior to the development of leukaemia. However the oligoclonal nature of the tumors
234 suggests a second hit – possibly leading to activation of an already over-expressed Notch1
235 receptor. To examine this possibility we sequenced the PEST and HD domains of *Notch1* in
236 thymic tumors from 12 dKO mice. One PEST domain mutation was detected (insertion C at
237 amino acid position 2421 leading to frame-shift and premature stop). Three HD mutations,
238 reported previously in both human and mouse T-ALL, were found (all T to C in residue 1668)
239 which result in a leucine to proline switch²⁵. Thus *Notch1* mutation was found in a minority
240 of tumors and predominantly affected the HD (25%) rather than the PEST domain (8%).

241

242

243 **Tumors are Notch1-dependent and killed by ZFP36L1 re-expression**

244 To establish if tumors were Notch-dependent we cultured primary tumor cells from dKO mice
245 on OP9-DL1 stromal cells in the presence of increasing concentrations of the gamma-
246 secretase inhibitor compound E which inhibits Notch signaling. After 72 hours cells were
247 counted and analysed by flow cytometry (**Fig. 5a**). Tumor growth was clearly sensitive to
248 compound E which was effective at concentrations as low as 0.1 μ M. To establish if tumor
249 development was Notch1-dependent *in vivo* we treated 12-week old mice with a Notch1
250 blocking antibody or saline control. This antibody is directed against the extracellular
251 negative regulatory region of Notch1 and stabilises its inactive state²⁶. In control mice
252 receiving the Notch1 blocking antibody thymic cellularity was reduced to <1% of normal and
253 this consisted predominantly of mature CD4 and CD8 single positive cells (**Fig. 5b,c**). This
254 demonstrated the ability of the antibody to block Notch1 signaling. Of the dKO mice
255 receiving saline injections, thymic tumors were seen in two (20%) and all showed grossly
256 abnormal thymic populations by flow cytometry (**Fig. 5c**). No tumors were seen in dKO mice
257 receiving the Notch1 blocking antibody and most had thymic cellularity <1% of normal. Two
258 mice in this cohort had an apparently enlarged thymus that consisted of predominantly
259 necrotic cells. We consider it likely that these represent pre-existing thymic tumors that were
260 killed by Notch1 blockade. Notch1 antibody treatment also led to the disappearance of
261 CD8⁺CD4⁻CD24^{hi}cTCR- β ⁻ and the CD8⁺CD4⁻CD24^{hi}cTCR- β ⁺ populations in the dKO mice
262 (**Fig. 5c**) indicating the expansion or maintenance of these cells *in vivo* was Notch1
263 dependent.

264 To establish the effect of re-expression of ZFP36L1 upon tumors cultured *in vitro*, primary
265 tumor cells were cultured on OP9-DL1 and then infected with equivalent titres of retrovirus
266 expressing green fluorescent protein (GFP) and either *ZFP36L1* or the Tandem zinc finger
267 mutant of *ZFP36L1*. Remarkably, ZFP36L1-expressing cells were almost completely
268 depleted from cultures confirming that expression of ZFP36L1 is toxic to primary tumor cells
269 (**Fig. 5d**). Taken together, these results suggest that the growth and survival of dKO tumor
270 cells remain dependent upon active Notch1 signaling and upon the absence of ZFP36L1.

271

272

273 **Discussion**

274

275 Current models of thymocyte development focus predominantly upon regulation of gene
276 expression at the level of the transcription factor. Recently a role for post-transcriptional
277 regulation of gene expression has been proposed in the context of microRNA²⁷. However
278 post-transcriptional regulation is also mediated by RBPs. To date, our greatest

279 understanding of RBPs has been their ability to regulate the stability of mRNA encoding
280 short-lived cytokines involved in the inflammatory response. Our knowledge of their role
281 during lymphocyte development is limited to a single report describing defective egress of
282 mature thymocytes from the thymus of mice deleted for the RBP *Elavl1*²⁸. Therefore the
283 data presented here establish a novel requirement for ZFP36L1 and ZFP36L2 during normal
284 thymic development. Furthermore they provide clear evidence of a critical role for ZFP36L1
285 and ZFP36L2 in the prevention of lymphoid malignancy.

286 Close to 100% of *Zfp36l1-Zfp36l2* dKO mice developed T-ALL, beginning from the age of
287 three months. This phenotype is seen only in dKO mice and never in any intermediate
288 combination of genotypes suggesting a high degree of redundancy between these two
289 highly homologous proteins. The evolutionary need for such redundancy is consistent with
290 the critical role demonstrated here in the prevention of malignancy. The absence of
291 leukaemia from any genotype other than the dKO is evidence against the phenotype being
292 due to an artefact of gene targeting. The toxicity of ZFP36L1, when re-expressed in tumor
293 cells, is further evidence that the leukaemic phenotype does indeed result from the loss of
294 ZFP36L1 and ZFP36L2. The involvement of ZFP36 family members in malignancy has
295 been previously suggested²⁰. Expression of ZFP36 family members is suppressed in a
296 range of human cancers and a tumor suppressor role has been proposed to act through
297 regulation of proliferative and anti-apoptotic factors^{17, 20}. However this is the first example in
298 which the intentional deletion of an RBP leads to the development of malignancy.

299 Prior to the development of T-ALL, thymic development is perturbed. In particular,
300 thymocytes appear able to bypass β -selection in the absence of a functional TCR- β chain.
301 In *Rag 1* and *2* dKO or TCR- β KO mice, DP differentiation can be partially rescued by
302 deletion of *Izklf1*, *Tcf3* or *Trp53*, or by the transgenic over-expression of *Ras*, *Map2k1* or
303 *Notch1*²⁹⁻³². However, *Zfp36l1-Zfp36l2* dKO thymocytes are clearly able to recombine the
304 TCR- β chain yet appear to be unable to suppress the developmental progression of TCR- β
305 negative thymocytes. Over-expression of *Notch1* in dKO mice might contribute to this
306 aspect of the phenotype. The increased metabolic activity of double negative thymocytes is
307 also consistent with increased expression of *Notch1* which is known to promote cellular
308 metabolism in cells at the stage of β -selection³³. Importantly, CD98 and CD71 expression in
309 normal thymocytes is promoted in a *Notch1*-dependent manner²³. This proves further
310 evidence that, in the absence of both ZFP36L1 and ZFP36L2, *Notch1* activity is abnormally
311 elevated in double negative thymocytes.

312 The over-expression of *Notch1*, observed prior to and after the development of leukaemia, is
313 also intriguing as chimeric mice reconstituted with bone marrow transduced with retrovirus

314 expressing Notch1-intracellular domain, and other mouse models that overexpress Notch1
315 invariably develop T-ALL^{24, 34-36}. The observed phenotype of Notch1-driven T-ALL typically
316 corresponds to the CD8iSP and DP stages of thymocyte development and closely
317 resembles the T-ALL seen in *Zfp36l1-Zfp36l2* dKO mice. The expansion of CD8iSP cells
318 was Notch1-dependent in the dKO mice prior to the onset of T-ALL. The results of luciferase
319 and EMSA experiments suggest that the elevated Notch1 expression is likely to result from
320 alleviation of ZFP36L1 and ZFP36L2-mediated suppression. Regulation of *Notch1* at the
321 post-transcriptional level has been proposed previously in the context of leech
322 development³⁷ but has not been proposed in the context of thymic development. The
323 degree of elevation of Notch1 in dKO mice prior to onset of leukaemia is modest – about
324 two-fold. However we consider this elevation significant because *Notch1* is normally
325 extremely tightly regulated both at the level of transcription and protein stability. The Notch
326 signaling pathway contains no amplification stage, therefore one ligand-receptor
327 engagement leads to one molecule of Notch intracellular domain complexing with a single
328 promoter and activating transcription from a single target allele. Notch1 is also unusual in
329 that a thymic phenotype has been described in the context of haplo-insufficiency³⁸. These
330 factors suggest that the Notch1 signaling pathway has evolved to regulate its expression
331 within very tight limits.

332 Importantly, overexpression of Notch1 has the capacity to contribute to both the leukaemic
333 phenotype and the aberrant β -selection^{24, 31}. This contribution of Notch1 to the leukaemic
334 phenotype is evidenced by the Notch1-dependency of tumor cells both *in vivo* and *in vitro*.
335 However, it is unclear whether the degree of elevation is, by itself, sufficient to initiate
336 leukaemia formation. The oligoclonal nature of the tumors suggests a “second hit”. This
337 might be mutation of the *Notch1* gene itself leading to the co-operative activation of the
338 Notch1 receptor that is already over-expressed in dKO thymocytes. It is also likely that
339 further unidentified ZFP36L1 and ZFP36L2 targets exist that contribute to the leukemic
340 phenotype. We chose to pursue *Notch1* because of its established role in thymic
341 development and the presence of predicted ZFP36L1 and ZFP36L2 binding sites in the
342 3’UTR. However ZFP36 family members are promiscuous in their binding requirements and
343 targets might exist that do not possess the classic AU-rich nonamer¹². Furthermore, our
344 microarray experiment would not have detected target genes regulated purely at the level of
345 translation. It is recognised that both microRNA and RBP frequently regulate multiple target
346 mRNA that encode genes with similar functions – so called “RNA regulons”³⁹. Therefore
347 Notch1 might represent one component of a co-ordinated program of gene expression
348 (normally suppressed by ZFP36L1 and ZFP36L2) that regulates the “activation status” of

349 developing thymocytes and, in the absence of ZFP36L1 and ZFP36L2, act together to
350 promote the leukemic phenotype.

351 While we show here that ZFP36L1 and ZFP36L2 are able to regulate expression of Notch1 it
352 is interesting that *Zfp36l2* has previously been identified as a gene positively regulated by
353 Notch1, suggesting that Notch1 induces the expression of its own negative regulator⁴⁰. This
354 is consistent with the mRNA expression pattern of *Zfp36l1* and *Zfp36l2* which are high during
355 the early DN stages but fall at the DN4 stage concurrent with a fall in Notch1 levels.
356 ZFP36L1 and ZFP36L2 are also regulated post-translationally and their activity is
357 suppressed by phosphorylation, by protein kinase B and by MAPKAP2⁴¹⁻⁴³. There is
358 considerable evidence of interplay between the PI3K and Notch signaling pathways and
359 phosphorylation of ZFP36L1 and ZFP36L2 might provide a further mechanism by which
360 PI3K activity is able to increase Notch1 expression⁴⁴⁻⁴⁵. Both the PI3K and MAP kinase
361 signaling pathways play a crucial role during thymocyte development; in addition to their
362 established roles this could additionally reflect their ability to regulate gene expression at the
363 post-transcriptional level by controlling the activity of RBPs such as ZFP36L1 and ZFP36L2.
364 The instantaneous and reversible manner in which ZFP36L1 and ZFP36L2 activity can be
365 regulated by phosphorylation is well suited to the changes in gene expression required
366 during thymocyte development. This would provide a mechanism whereby PI3K or MAPK
367 activity could effect rapid changes in expression of transcription factors such as Notch1,
368 thereby integrating extracellular cues with both post-transcriptional and transcriptional
369 control of gene expression.

370 Our finding that *Notch1* can be regulated at the RNA level is of potentially great significance
371 to human disease. *NOTCH1* is mutated in >50% human T-ALL and co-operating mutations
372 affecting both HD and PEST domains are frequent⁴⁶. Truncation of the 3'UTR as a result of
373 alternative polyadenylation site usage is commonly seen in malignancy and it is plausible
374 that mutation or truncation of the *NOTCH1* 3'UTR might co-operate with coding sequence
375 mutations to further increase NOTCH1 activity. Preliminary experiments involving analysis
376 of array CGH (aCGH) data from 69 human T-ALL samples identified recurrent deletions in
377 chromosome 14q24 including the *ZFP36L1* locus in 3 cases. This finding is intriguing, but of
378 uncertain significance as these were non-focal, heterozygous deletions encompassing
379 several additional genes besides *ZFP36L1*. No genetic alterations involving *ZFP36L2* in
380 chromosome 2 were present in this series. However, many alternative mechanisms might
381 lead to suppression of ZFP36L1 and ZFP36L2 activity including epigenetic or post-
382 translational modification by altered kinase or phosphatase activity in leukaemic cells.
383 Similarly, defects downstream of ZFP36L1 or ZFP36L2 in the RNA regulation pathway might
384 contribute to the pathogenesis of human malignancy.

385

386 In summary, these data reveal a critical role for the RNA-binding proteins ZFP36L1 and
387 ZFP36L2 during thymocyte development. They highlight the significant impact of post-
388 transcriptional regulation of gene expression during thymic development. Furthermore, they
389 also demonstrate a critical role for these proteins as tumor suppressors in the prevention of
390 malignant transformation.

391

392 **Accession codes:** Microarray data has been submitted to the European Bioinformatics
393 Institute ArrayExpress database, accession number E-MEXP-2737.

394 **Acknowledgements**

395 We thank all of our colleagues for their input during the preparation of this manuscript.
396 D.J.H. was funded by a fellowship from Cancer Research UK and by the Addenbrooke's
397 Charitable Trust. A.G. is supported by a MRC CASE studentship. M.T. is a Medical
398 Research Council Senior Non-Clinical Fellow and also received funding for this work from
399 BBSRC grant number BB/C506121/1. This work was supported by the National Institutes of
400 Health grants R01CA120196 and R01CA129382 to A.F and the ECOG tumor bank grant
401 U24 CA114737. A. F. is a Leukemia & Lymphoma Society Scholar. K. D. K. is a postdoctoral
402 researcher funded by the "Fonds voor Wetenschappelijk Onderzoek-Vlaanderen" and
403 recipient of a Belgian American Educational Foundation (BAEF) fellowship.

404

405 **AUTHOR CONTRIBUTIONS**

406 D.J.H. designed and performed experiments, analysed data and wrote the paper; M.J., A.G.,
407 S.E.B., designed and performed experiments; C.M.L., R.P., G.G., C.W.S. and H.R.M.
408 developed analytical tools; S.A. designed experiments, analysed data; M.T. designed
409 experiments, analysed data and wrote the paper.

410

411 **COMPETING INTERESTS STATEMENT**

412 C.W.S. was employed by Genentech Inc. during the course of this study.

413

414

415 **Figure legends**

416

417 **Figure 1. *Zfp36l1-Zfp36l2* dKO mice develop T-ALL.**

418 A. Kaplan Meier Survival of dKO (red line, n=37), *Zfp36l2* single knockout (dashed line,
419 n=14) and control (blue line, n=30) mice. B. Flow cytometric analysis of control thymus and a
420 dKO thymic tumor stained with indicated antibodies. sTCR- β = surface TCR- β , icTCR- β =
421 intracellular TCR- β . Solid red line = icTCR- β , broken blue line = isotype control. C. Low
422 power examination of peripheral blood from diseased dKO mouse showing leukocytosis. D.
423 High power examination of peripheral blood from diseased dKO mouse showing circulating
424 lymphoblasts. E. Flow cytometric analysis of thymus, spleen and marrow from a
425 representative control and a diseased dKO mouse. F. D β 2-J β 2 rearrangement by PCR of
426 DNA from control kidney, three control thymi, five dKO thymi (12-weeks old) and four dKO
427 thymic tumors.

428

429 **Figure 2 Thymocyte development is perturbed prior to tumor development**

430 A. Flow cytometric plots gated on cells negative for dump channel (B220, Ter119, NK1.1, $\gamma\delta$ -
431 TCR, Mac-1, Gr1). B. Total thymic cellularity showing thymic atrophy in dKO mice.
432 Statistical analysis used Mann-Whitney test. C. Flow cytometric plots gated on CD8 single
433 positive population (CD8⁺CD4⁻ as shown in A) showing proportions of immature
434 (CD24^{hi}sTCR β ⁻) and mature (CD24^{int}sTCR β ⁺) CD8 single positive thymocytes. D. Immature
435 CD8 single positive thymocytes as a percentage of all CD8 SP cells (upper) or absolute
436 number per thymus (lower) at the indicated age of mice. Graphs show the mean and SEM
437 for five mice per genotype. E. Flow cytometric plots from 3-week old mice gated on dump
438 channel negative, CD4⁻CD8⁻ double negative thymocytes. For all flow cytometric plots
439 numbers show the percentage of cells within the indicated gate and represent the mean from
440 one experiment of 4-5 mice per genotype. All plots are representative of at least nine
441 individual mice.

442

443 **Figure 3 Expression of Notch1 is elevated in *Zfp36l1-Zfp36l2* dKO mice**

444 A. Heatmap summary of microarray performed on cDNA from whole thymus of control and
445 dKO mice at five and nine weeks of age. Criteria for inclusion are genes changing
446 significantly (p<0.05), elevated > 1.5 fold in dKO mice at both five weeks and nine weeks
447 relative to control thymus. B. Real-time PCR performed upon cDNA from whole thymus for
448 *Notch1* and *Notch* target genes. Values are normalised to expression of *B2m* and presented

449 relative to expression of each gene in thymocytes from control mice. Graphs show mean and
450 SEM of 3-8 mice. C. Immunoblot for the cleaved intracellular Notch1 (iCN1) performed on
451 whole thymus from control or diseased double knockout mice. D. Notch1 mean
452 fluorescence intensity (MFI) by flow cytometry (normalised to isotype control) in control
453 thymus and dKO thymic tumors. E. Notch1 expression in double negative, double positive,
454 CD8 and CD4 populations using the gating strategy shown. Mean and SEM are shown for
455 five separate thymic tumors. F. Notch1 expression by flow cytometry on thymocyte
456 populations gated as shown in 3-week old. Upper plots are gated on dump channel (B220,
457 Ter119, NK1.1, $\gamma\delta$ -TCR, Mac-1, Gr1) negative. Lower plots gated on dump⁻CD4⁻CD8⁻ DN
458 thymocytes and show the gating of populations A, B & C. G. Notch1 expression by flow
459 cytometry in CD8 subpopulations (D, E & F) from 3-week old mice using gating strategy
460 indicated. Unless stated, error bars show the mean and standard error of four-five mice per
461 genotype. Statistical analysis performed using Mann Whitney test. (* $P < 0.05$, ** $P < 0.01$)
462

463 **Figure 4 ZFP36L1 and ZFP36L2 exert suppression via interaction with sequences in**
464 **the Notch1 3'UTR.**

465 **A.** *Notch1* 3'UTR presented as degree of conservation between human and mouse using
466 the Vista Genome Browser. The highly conserved region (HCR) of interest is underlined in
467 red. **B.** Detailed view showing inter-species sequence conservation for the underlined
468 region in A. Black background indicates 100% conservation between human, mouse, dog,
469 armadillo, opossum and platypus. Predicted ZFP36L1 and ZFP36L2 binding sites are boxed
470 in red. **C.** Luciferase reporters were constructed corresponding to the full length *Notch1*
471 3'UTR (N1 UTR full length), the proximal HCR underlined in red in A (N1 HCR), or the
472 *Notch1* 3'UTR with the HCR removed (N1 Δ HCR). These reporters were co-transfected
473 into HEK293T cells along with a pCDNA3 empty control vector or pCDNA3 expressing
474 *ZFP36L1*, *ZFP36L2* or a tandem zinc finger mutant of *ZFP36L1* (TZFM). Results are shown
475 as the mean and SEM of five separate transfections and are representative of three
476 experiments. Statistical analysis performed by ANOVA with Tukey post-hoc analysis (* $P <$
477 0.001) **D.** Titration of transfected *ZFP36L1* or *ZFP36L2*. Mean and SEM of five separate
478 transfections are shown. **E.** Electromobility shift assay (EMSA) following incubation of a
479 radiolabelled *Notch1* probe (corresponding to the 61 nucleotides containing the nonameric
480 AU sequence) with lysates from 293T cells transfected with the indicated expression
481 constructs. pCDNA3 = empty control vector, TZFM = tandem zinc finger mutant.

482

483

484

485 **Figure 5 Inhibition of Notch or re-expression of ZFP36L1 is toxic to tumor growth**
486 **A.** Primary dKO tumor cells were cultured on OP9-DL1 stromal cells for three days in the
487 presence of increasing concentrations of the gamma-secretase inhibitor Compound E.
488 Graph shows mean and SEM for six tumors presented relative to the number of cells
489 seeded. Statistical analysis was performed by repeated measures ANOVA with Tukey post
490 hoc analysis. (**p<0.01, ***p<0.001) **B.** Notch1 blocking antibody, or saline control, was
491 administered *in vivo* to 11 week old control and dKO mice. After three weeks of treatment
492 thymus was analysed by flow cytometry. Post-treatment thymic cellularity is shown for
493 individual mice. **C.** Representative flow cytometry plots of thymus after treatment with
494 control or Notch1 blocking antibody. CD4-8 plots are gated on thymocytes negative for
495 B220, NK1.1, $\gamma\delta$ -TCR, mac-1, Gr1, Ter119. CD24-icTCR- β plots are gated on the CD8
496 single positive quadrant. **D.** Primary thymic tumors from dKO mice were cultured on OP9-
497 DL1 stromal cells for 24 hours before infection with equivalent titres of retrovirus expressing
498 either *ZFP36L1* or the tandem zinc finger mutant of *ZFP36L1* (TZFM). After three days cells
499 were analysed by flow cytometry. Flow cytometry plots shown are representative of infection
500 of five separate dKO tumors.

501

502

503

504

505

506 **Online Methods**

507 **Mice**

508 All procedures involving mice were approved by the U.K. Home Office and the Babraham
509 Institute Animal Welfare and Experimentation Committee.

510

511 **Gene Targeting**

512 The *Zfp36l1* and *Zfp36l2* targeting vectors were generated by inserting LoxP sites either side
513 of exon 2. Correctly targeted embryonic stem cell clones were identified by Southern
514 blotting using both 3' and 5' flanking probes. Chimeras were generated by standard
515 techniques. Mice were bred to FlpE deleter mice to remove the neomycin cassette⁴⁷. Mice
516 were then bred to CD2-Cre transgenic mice. Genotyping was performed using primers listed
517 in **Supplementary table 1**.

518

519 **Flow cytometry analysis**

520 Cell suspensions were stained for 30 minutes using antibodies detailed below. For
521 intracellular staining cells were fixed using CytofixCytoperm (BD) and stained for one hour at
522 room temperature in PermWash buffer (BD). FACS data was acquired on an LSRII (BD)
523 and analyzed using FlowJo software (TreeStar).

524

525 **Flow sorting**

526 Double negative thymic populations were pre-enriched by negative MACS depletion. Cell
527 suspensions were incubated with anti-CD8 biotin, followed by anti-biotin MicroBeads
528 (Miltenyi Biotech) and then applied to MACS separation columns (Miltenyi Biotech). Cells
529 were then stained for CD44, CD25, CD98 and a dump channel (CD4, CD8, TER119, Mac1,
530 Gr1, B220, NK1.1, $\gamma\delta$ TCR). Cells were sorted on a FACSAria (BD): DN1 (CD44⁺CD25⁻),
531 DN2 (CD44⁺CD25⁺), DN3 (CD44⁻CD25⁺CD98⁻) and DN4 (CD44⁻CD25⁻CD98⁺). CD8
532 populations were sorted following MACS depletion of CD4 then sorted based on: CD8iSP
533 (CD8⁺sTCR- β ⁻CD24^{hi}) CD8mSP (CD8⁺sTCR- β ⁺CD24^{int}). CD4 and DP populations were
534 sorted by expression of CD4 and CD8.

535

536 **Antibodies for flow cytometry and immunoblotting**

537 Biotin-Gr1(RB6-8C5), Biotin-NK1.1 (PK136), Biotin- $\gamma\delta$ -TCR (GL3), FITC-CD25 (7D4),
538 PerCP-Cy5.5-CD8 α (53-6.7), PE-CD98 (RL388) and FITC-CD24 (M1/69) were purchased
539 from BD. PE-Cy7-CD4 (L3T4), PECy5.5-CD44 (IM7), PE-CD71 (R17217), PE-TCR- β (H57-
540 597), Biotin-TER119, Biotin-B220 (RA3-6B2) were purchased from eBioscience. Biotin-
541 CD11b (RM2815) was purchased from Caltag. Notch1 staining was performed using PE-

542 Notch1 (mN1A) from BD and Biotin-Notch1 rat IgG2a (22E5.5)⁴⁸. For immunoblotting
543 BRf1/2(#2119) and Cleaved Notch1 (Val1744) (D3B8) were purchased from Cell Signaling
544 Technology. The EdU staining kit was purchased from Invitrogen and used as per the
545 manufacturer's instructions.

546

547 **Microarray**

548 Samples were prepared from thymus in Trizol (Invitrogen). RNA was extracted using the
549 RNEasy kit (Qiagen) including the on column DNase step. Expression profiling was
550 performed using Affymetrix mouse gene ST1.0 array and analysed using Genespring
551 software. Raw data was subjected to RMA normalisation. Probes whose raw intensity fell
552 into the bottom 20% of every replicate across all conditions were removed as being
553 unexpressed. The remaining probes were tested separately for a significant change in
554 expression between control and either 5 or 9 weeks using an unpaired t-test with a cut-off of
555 $p < 0.05$ after applying a Benjamini and Hochberg multiple testing correction. The
556 significantly changing genes were further filtered to remove any with an absolute change of
557 < 1.5 fold between conditions.

558

559 **TCR- β 2 Clonality PCR**

560 PCR primers were used as previously described⁴⁹.

561

562 **RT-PCR**

563 cDNA was synthesised from RNA using Superscript II (Invitrogen). RT-PCR was performed
564 using Platinum QPCR mix (Invitrogen) and primers detailed in **Supplementary table 1** and
565 run on a Chromo4 analyser (MJ Research). Results were normalised to the reference genes
566 B2M or to GAPDH as indicated in text. See **supplementary table 1** for primer sequences.
567 B2M and GAPDH assay were purchased from ABI.

568

569 **Plasmid Constructs**

570 pcDNA3.myc.WT *ZFP36L1* expression construct and pFLAG.CMV2-*ZFP36L2* were obtained
571 from Dr Andrew Clark (Kennedy Institute of Rheumatology, London). The *ZFP36L1* tandem
572 zinc finger mutant (TZFM) C135/173R was made by site directed mutagenesis. See
573 **Supplementary table 1** for primer sequences. The *ZFP36L1* and *ZFP36L2* coding
574 sequences, generated by PCR from the constructs, above were cloned into the MIGRI
575 retroviral vector using the BglII and EcoRI sites. The mouse *Notch1* 3'UTR reporters were
576 cloned from CHORI BAC clone RP23-306D20 into pSI-Check2 (Promega). See
577 **Supplementary table 1** for primer sequences.

578

579 **Luciferase assays**

580 293T cells were cultured in DMEM, 10% FCS, 2mM Glutamine and 100 U/ml
581 Penicillin/Streptomycin then transfected with luciferase reporter (20 ng) plus *ZFP36L1* or
582 *ZFP36L2* expression vector (0.3 – 2.5 ng) using the CalPhos kit (Clontech). Firefly and
583 Renilla luciferase activity was analyzed 24 hours post transfection using the Dual-Glo
584 luciferase reporter assay system (Promega) and analyzed on a TopCount NXT microplate
585 luminescence counter.

586

587 **EMSA**

588 Complimentary oligonucleotides incorporating a T7 promoter and 61 nucleotides of the
589 Notch1 3'UTR HCR were used for in vitro transcription of ³²P labelled RNA probe using the
590 T7 Maxiscript kit (Ambion). 200 fmol of radiolabelled probe was incubated with 20 µg of
591 lysate from transfected 293T cells for 20' at room temperature followed by incubation with
592 5mg/ml heparin and 50U/ml RNase T1. Protein-RNA complexes were resolved on a 4.5%
593 acrylamide in 0.5X TBE gel then exposed to a Fuji Phosphoimager screen.

594

595 **Tumor culture**

596 Primary tumor cells were seeded onto OP9-DL1 stromal cells (provided by Dr Zuniga-
597 Pflucker, University of Toronto) in α -MEM, 20% FCS, 2mM Glutamine and 100 U/ml
598 Penicillin-Streptomycin. Compound-E was from Alexis Biochemicals. Retroviral supernatant
599 was produced by transfection of Platinum-E packaging cells and titrated on 3T3 fibroblasts.
600 Tumor cells were infected with retroviral supernatant in the presence of 5µg/ml Polybrene
601 (Sigma) and centrifuged at 2500 rpm for 30 minutes.

602

603 ***In vivo* Notch1 blocking experiments**

604 Notch1 Blocking antibody was administered by intraperitoneal injection twice weekly for 3
605 weeks at a dose of 5mg/kg²⁶.

606

607 **Statistics**

608 Statistical analysis was performed using InStat-3 software (GraphPad, San Diego, CA).
609 Tests used were Mann-Whitney and ANOVA with post-hoc analysis by Tukey.

610

611 **Sequencing**

612 Sequencing of Notch1 was performed as described ²⁵.

613

614 **Array CGH analysis**

615 Leukemic DNA and cryopreserved lymphoblast samples were provided by collaborating
616 institutions in the US [Eastern Cooperative Oncology Group (ECOG) and Pediatric Oncology
617 Group (POG)]. All samples were collected in clinical trials with informed consent and under
618 the supervision of local IRB committees. Consent was obtained from all patients at trial entry
619 according to the Declaration of Helsinki. T-cell phenotype was confirmed by flow cytometry.
620 Array-CGH analysis of human T-ALLs was performed with SurePrint G3 Human CGH 1x1M
621 Oligo Microarrays (Agilent Technologies) according to the instructions of the manufacturer
622 using a commercial normal DNA as reference (Promega). Array CGH data was analyzed
623 with the Genomic Workbench 5.0.14 software (Agilent Technologies).

624

625

626

627

628

629

630

631 **References**

632

- 633 1. Georgescu, C. *et al.* A gene regulatory network armature for T lymphocyte specification.
634 *Proc. Natl. Acad. Sci. U. S. A.* **105**, 20100-20105 (2008).
- 635 2. Rothenberg, E.V. Negotiation of the T lineage fate decision by transcription-factor interplay
636 and microenvironmental signals. *Immunity* **26**, 690-702 (2007).
- 637 3. Rothenberg, E.V., Moore, J.E. & Yui, M.A. Launching the T-cell-lineage developmental
638 programme. *Nat Rev Immunol* **8**, 9-21 (2008).
- 639 4. Galante, P.A. *et al.* A comprehensive in silico expression analysis of RNA binding proteins in
640 normal and tumor tissue: Identification of potential players in tumor formation. *RNA Biol* **6**,
641 426-433 (2009).
- 642 5. Taylor, G.A. *et al.* A pathogenetic role for TNF alpha in the syndrome of cachexia, arthritis,
643 and autoimmunity resulting from tristetraprolin (TTP) deficiency. *Immunity* **4**, 445-454
644 (1996).
- 645 6. Carballo, E., Lai, W.S. & Blakeshear, P.J. Feedback inhibition of macrophage tumor necrosis
646 factor-alpha production by tristetraprolin. *Science* **281**, 1001-1005 (1998).
- 647 7. Bell, S.E. *et al.* The RNA binding protein Zfp3611 is required for normal vascularisation and
648 post-transcriptionally regulates VEGF expression. *Dev. Dyn.* **235**, 3144-3155 (2006).
- 649 8. Stumpo, D.J. *et al.* Chorioallantoic fusion defects and embryonic lethality resulting from
650 disruption of Zfp36L1, a gene encoding a CCCH tandem zinc finger protein of the
651 Tristetraprolin family. *Mol. Cell. Biol.* **24**, 6445-6455 (2004).
- 652 9. Stumpo, D.J. *et al.* Targeted disruption of Zfp3612, encoding a CCCH tandem zinc finger RNA-
653 binding protein, results in defective hematopoiesis. *Blood* **114**, 2401-2410 (2009).
- 654 10. Blakeshear, P.J. *et al.* Characteristics of the interaction of a synthetic human tristetraprolin
655 tandem zinc finger peptide with AU-rich element-containing RNA substrates. *J. Biol. Chem.*
656 **278**, 19947-19955 (2003).
- 657 11. Hudson, B.P., Martinez-Yamout, M.A., Dyson, H.J. & Wright, P.E. Recognition of the mRNA
658 AU-rich element by the zinc finger domain of TIS11d. *Nat Struct Mol Biol* **11**, 257-264 (2004).
- 659 12. Emmons, J. *et al.* Identification of TTP mRNA targets in human dendritic cells reveals TTP as a
660 critical regulator of dendritic cell maturation. *RNA* **14**, 888-902 (2008).
- 661 13. Klein, U. *et al.* The DLEU2/miR-15a/16-1 cluster controls B cell proliferation and its deletion
662 leads to chronic lymphocytic leukemia. *Cancer Cell* **17**, 28-40 (2010).
- 663 14. Mayr, C. & Bartel, D.P. Widespread shortening of 3'UTRs by alternative cleavage and
664 polyadenylation activates oncogenes in cancer cells. *Cell* **138**, 673-684 (2009).
- 665 15. Wiestner, A. *et al.* Point mutations and genomic deletions in CCND1 create stable truncated
666 cyclin D1 mRNAs that are associated with increased proliferation rate and shorter survival.
667 *Blood* **109**, 4599-4606 (2007).
- 668 16. Sandberg, R., Neilson, J.R., Sarma, A., Sharp, P.A. & Burge, C.B. Proliferating cells express
669 mRNAs with shortened 3' untranslated regions and fewer microRNA target sites. *Science*
670 **320**, 1643-1647 (2008).
- 671 17. Brennan, S.E. *et al.* The mRNA-destabilizing protein tristetraprolin is suppressed in many
672 cancers, altering tumorigenic phenotypes and patient prognosis. *Cancer Res.* **69**, 5168-5176
673 (2009).
- 674 18. Jackson, R.S., 2nd, Cho, Y.J. & Liang, P. TIS11D is a candidate pro-apoptotic p53 target gene.
675 *Cell Cycle* **5**, 2889-2893 (2006).
- 676 19. Baou, M. *et al.* Involvement of Tis11b, an AU-rich binding protein, in induction of apoptosis
677 by rituximab in B cell chronic lymphocytic leukemia cells. *Leukemia* **23**, 986-989 (2009).
- 678 20. Benjamin, D. & Moroni, C. mRNA stability and cancer: an emerging link? *Expert Opin Biol*
679 *Ther* **7**, 1515-1529 (2007).

- 680 21. de Boer, J. *et al.* Transgenic mice with hematopoietic and lymphoid specific expression of
681 Cre. *Eur. J. Immunol.* **33**, 314-325 (2003).
- 682 22. Dumont, C. *et al.* Rac GTPases play critical roles in early T-cell development. *Blood* **113**,
683 3990-3998 (2009).
- 684 23. Kelly, A.P. *et al.* Notch-induced T cell development requires phosphoinositide-dependent
685 kinase 1. *EMBO J.* **26**, 3441-3450 (2007).
- 686 24. Demarest, R.M., Ratti, F. & Capobianco, A.J. It's T-ALL about Notch. *Oncogene* **27**, 5082-5091
687 (2008).
- 688 25. O'Neil, J. *et al.* Activating Notch1 mutations in mouse models of T-ALL. *Blood* **107**, 781-785
689 (2006).
- 690 26. Wu, Y. *et al.* Therapeutic antibody targeting of individual Notch receptors. *Nature* **464**, 1052-
691 1057 (2010).
- 692 27. O'Connell, R.M., Rao, D.S., Chaudhuri, A.A. & Baltimore, D. Physiological and pathological
693 roles for microRNAs in the immune system. *Nat Rev Immunol* **10**, 111-122 (2010).
- 694 28. Papadaki, O. *et al.* Control of thymic T cell maturation, deletion and egress by the RNA-
695 binding protein HuR. *J. Immunol.* **182**, 6779-6788 (2009).
- 696 29. Winandy, S., Wu, L., Wang, J.H. & Georgopoulos, K. Pre-T cell receptor (TCR) and TCR-
697 controlled checkpoints in T cell differentiation are set by Ikaros. *J. Exp. Med.* **190**, 1039-1048
698 (1999).
- 699 30. Michie, A.M. & Zuniga-Pflucker, J.C. Regulation of thymocyte differentiation: pre-TCR signals
700 and beta-selection. *Semin. Immunol.* **14**, 311-323 (2002).
- 701 31. Michie, A.M. *et al.* Constitutive Notch signalling promotes CD4 CD8 thymocyte
702 differentiation in the absence of the pre-TCR complex, by mimicking pre-TCR signals. *Int.*
703 *Immunol.* **19**, 1421-1430 (2007).
- 704 32. Campese, A.F. *et al.* Notch1-dependent lymphomagenesis is assisted by but does not
705 essentially require pre-TCR signaling. *Blood* **108**, 305-310 (2006).
- 706 33. Ciofani, M. & Zuniga-Pflucker, J.C. Notch promotes survival of pre-T cells at the beta-
707 selection checkpoint by regulating cellular metabolism. *Nat Immunol* **6**, 881-888 (2005).
- 708 34. Pear, W.S. *et al.* Exclusive development of T cell neoplasms in mice transplanted with bone
709 marrow expressing activated Notch alleles. *J. Exp. Med.* **183**, 2283-2291 (1996).
- 710 35. Aster, J.C., Pear, W.S. & Blacklow, S.C. Notch signaling in leukemia. *Annu Rev Pathol* **3**, 587-
711 613 (2008).
- 712 36. Li, X., Gounari, F., Protopopov, A., Khazaie, K. & von Boehmer, H. Oncogenesis of T-ALL and
713 nonmalignant consequences of overexpressing intracellular NOTCH1. *J. Exp. Med.* **205**, 2851-
714 2861 (2008).
- 715 37. Gonsalves, F.C. & Weisblat, D.A. MAPK regulation of maternal and zygotic Notch transcript
716 stability in early development. *Proc. Natl. Acad. Sci. U. S. A.* **104**, 531-536 (2007).
- 717 38. Washburn, T. *et al.* Notch activity influences the alphabeta versus gammadelta T cell lineage
718 decision. *Cell* **88**, 833-843 (1997).
- 719 39. Keene, J.D. RNA regulons: coordination of post-transcriptional events. *Nat Rev Genet* **8**, 533-
720 543 (2007).
- 721 40. Moellering, R.E. *et al.* Direct inhibition of the NOTCH transcription factor complex. *Nature*
722 **462**, 182-188 (2009).
- 723 41. Schmidlin, M. *et al.* The ARE-dependent mRNA-destabilizing activity of BRF1 is regulated by
724 protein kinase B. *EMBO J.* **23**, 4760-4769 (2004).
- 725 42. Benjamin, D., Schmidlin, M., Min, L., Gross, B. & Moroni, C. BRF1 protein turnover and mRNA
726 decay activity are regulated by protein kinase B at the same phosphorylation sites. *Mol. Cell.*
727 *Biol.* **26**, 9497-9507 (2006).
- 728 43. Maitra, S. *et al.* The AU-rich element mRNA decay-promoting activity of BRF1 is regulated by
729 mitogen-activated protein kinase-activated protein kinase 2. *RNA* **14**, 950-959 (2008).

730 44. Palomero, T. *et al.* Mutational loss of PTEN induces resistance to NOTCH1 inhibition in T-cell
731 leukemia. *Nat. Med.* **13**, 1203-1210 (2007).

732 45. Palomero, T., Dominguez, M. & Ferrando, A.A. The role of the PTEN/AKT Pathway in
733 NOTCH1-induced leukemia. *Cell Cycle* **7**, 965-970 (2008).

734 46. Weng, A.P. *et al.* Activating mutations of NOTCH1 in human T cell acute lymphoblastic
735 leukemia. *Science* **306**, 269-271 (2004).

736 47. Rodriguez, C.I. *et al.* High-efficiency deleter mice show that FLPe is an alternative to Cre-
737 loxP. *Nat. Genet.* **25**, 139-140 (2000).

738 48. Fiorini, E. *et al.* Dynamic regulation of notch 1 and notch 2 surface expression during T cell
739 development and activation revealed by novel monoclonal antibodies. *J. Immunol.* **183**,
740 7212-7222 (2009).

741 49. Dumortier, A. *et al.* Notch activation is an early and critical event during T-Cell
742 leukemogenesis in Ikaros-deficient mice. *Mol. Cell. Biol.* **26**, 209-220 (2006).

743

744

Figure 1

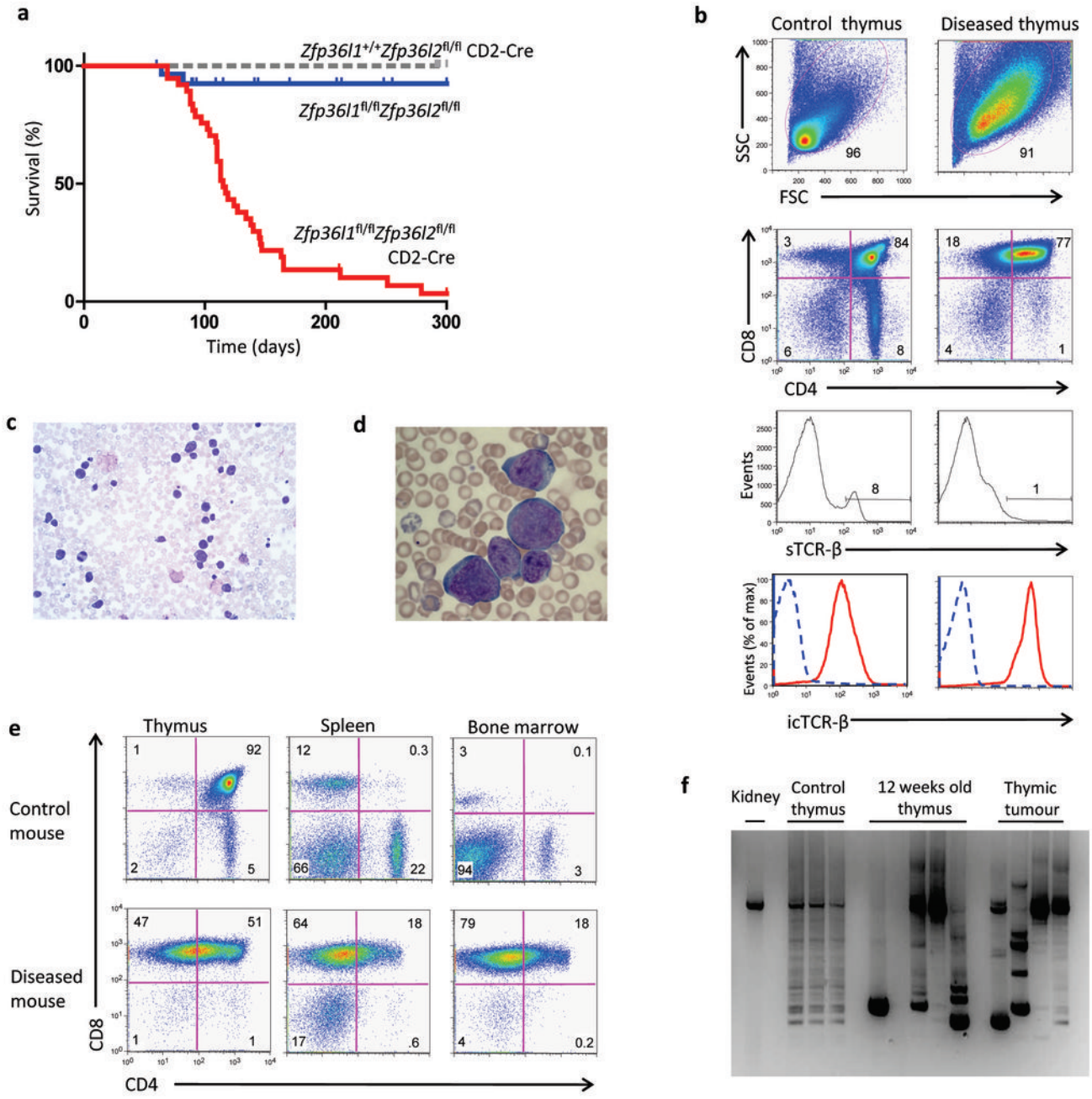


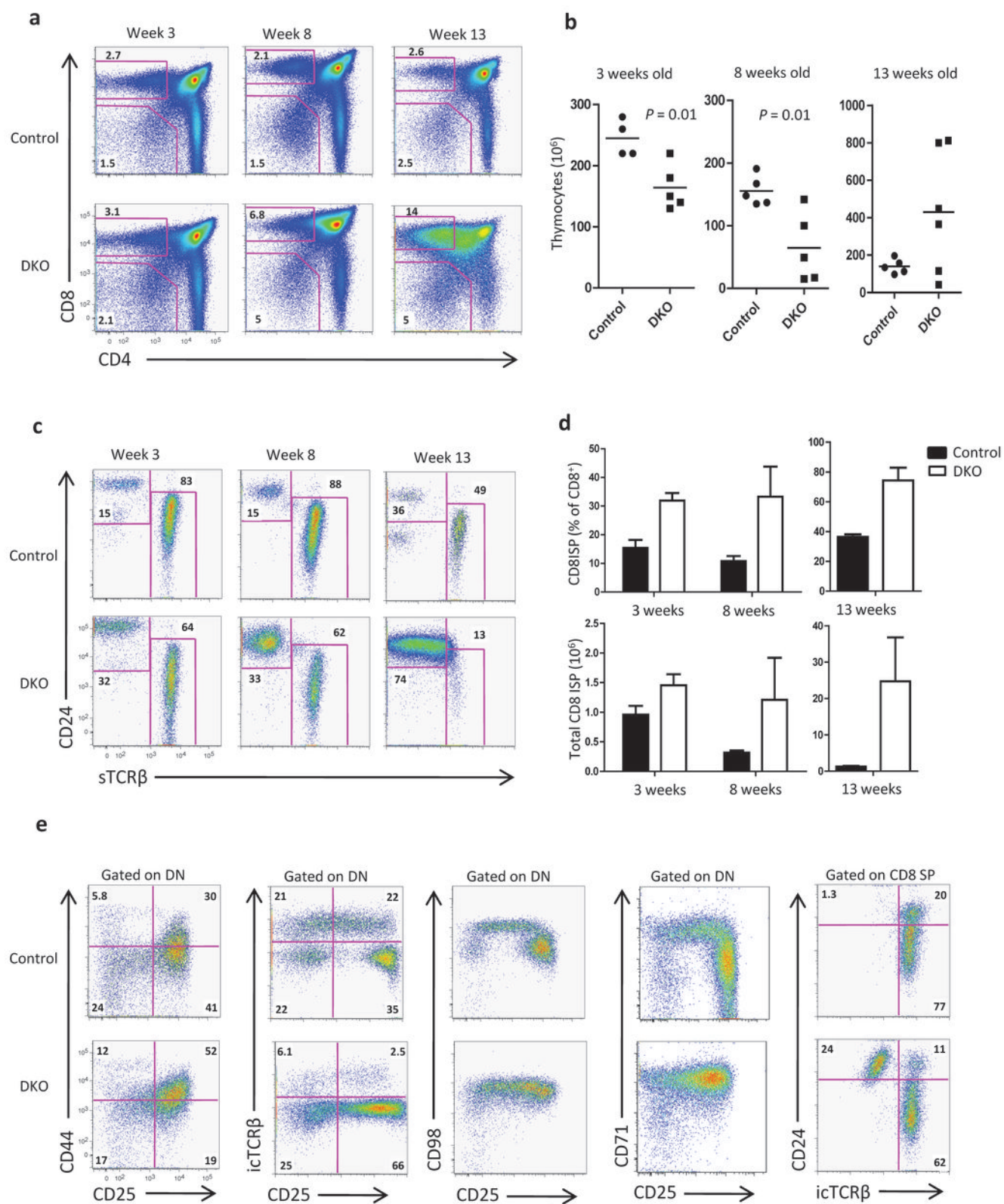
Figure 2

Figure 3

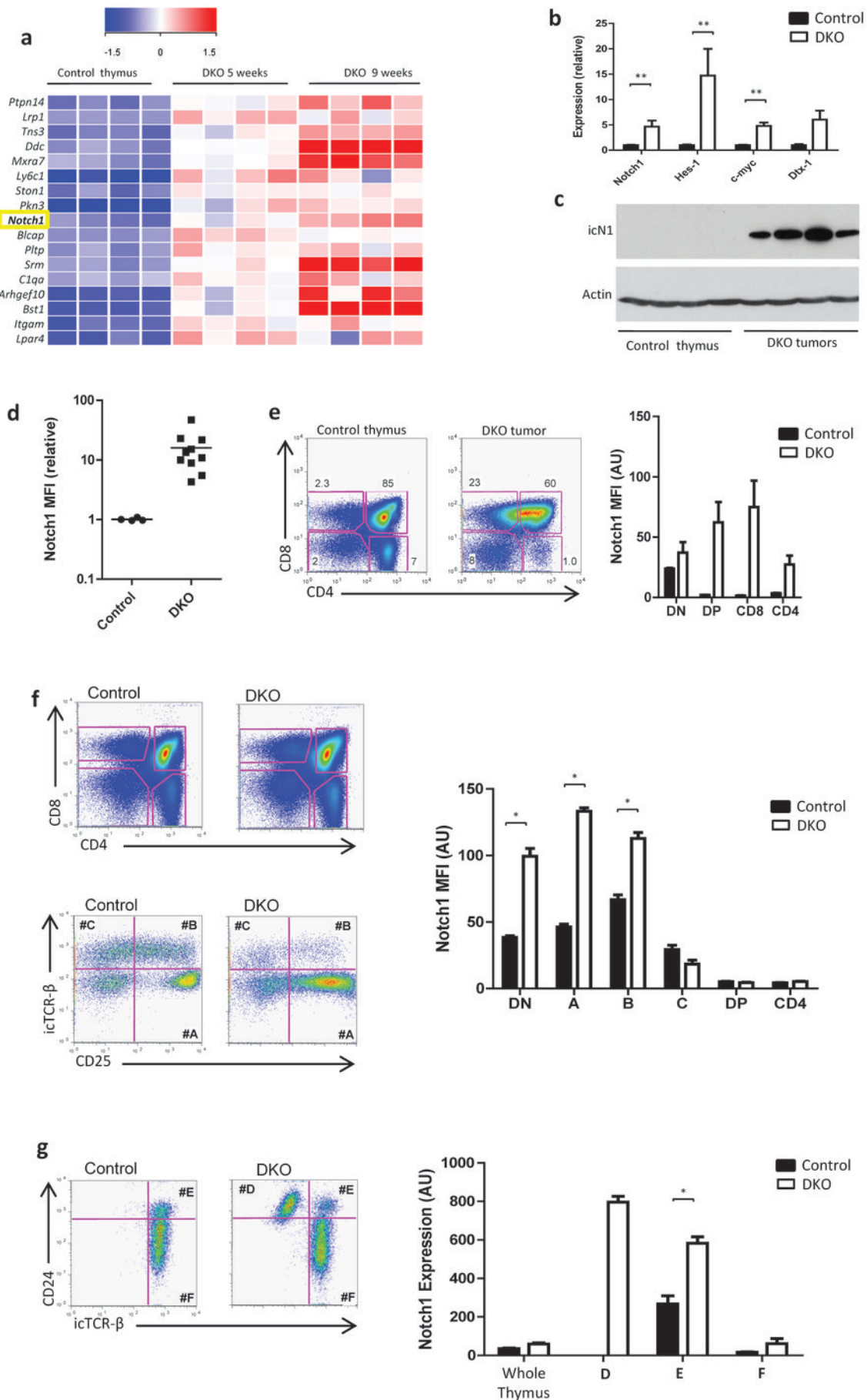


Figure 4

